

LASER APPLICATIONS AND OTHER TOPICS IN QUANTUM ELECTRONICS https://doi.org/10.1070/QEL17081

Physical processes affecting the survival of microbiological systems in laser printing of gel droplets

V.P. Zarubin, V.S. Zhigarkov, V.I. Yusupov, A.A. Karabutov

Abstract. **We consider laser printing of gel microdroplets – a promising method for microbiology, biotechnology and medicine. In the printing process, small volumes of gel containing living microorganisms are transferred as a result of cavitation caused by the absorption of a short laser pulse in a metal film. However, in such a transfer, certain physical factors arise that can lead to damage and death of biological material. These factors include elevated temperature and pressure, high radiation intensity and some others. Experimental estimates of these parameters are conducted, based on measurements of the acoustic response of laser printing, electron microscopy of the affected areas and the results of high-speed imaging of the transfer process. It is shown that these factors are not a significant limitation for the technology being developed. Laser printing is performed by exposing a metal film to laser pulses with an energy of 5–30 μJ and a duration of 8–14 ns, the laser beam diameter being 30 μm.**

Keywords: *laser pulsed action, acoustic signal, microorganisms, nanoparticles.*

1. Introduction

Many biological and medical applications of the laser-induced forward transfer process are currently being developed [1–16]. One of the newest applications is the isolation, or laser printing, of hard-to-cultivate microorganisms [17, 18]. In laser printing, a substrate layer (gel with cells or microorganisms) is applied to a donor glass plate with a thin absorbing metal coating [19–23]. Pulsed laser radiation is focused on the metal layer. Radiation absorption leads to rapid local heating of the metal film and to the appearance of a rapidly expanding vapour-gas bubble. As it expands, jets of liquid appear, transferring droplets with a small number of microscopic living systems onto an acceptor glass plate, a Petri dish, or into the wells of a tablet. The principal advantage of laser printing in microbiology and medicine is the possibility of targeted transfer of a given microscopic amount of matter (individual cells and their agglomerates). In this case, however, the conditions of the ongoing processes are quite stringent with respect to living organisms: there is a number of negative physical factors such as shock acoustic waves, high temperatures, high dynamic loads in the droplet transfer, toxic nanoparticles formed during the destruction of sections of the absorbing film and a high intensity of pulsed laser radiation transmitted through a metal film.

In this work, we evaluate the impact of these factors on the survival of microorganisms in the processes of laser printing of gel droplets. These estimates are important both for optimising the method and as an additional material in interpreting the results of biological experiments using laser printing.

2. Experimental setup

A schematic of the laser printing system for microbiological systems, described in detail in [24], is shown in Fig. 1. The radiation source is a YLPM-1-4x200-20-20 (LLC NTO IRE-Polyus, Russia) laser (*1*) with a radiation wavelength of 1064 nm, a pulse duration of 4–200 ns, and an energy of 2 μJ–1 mJ. To position the laser beam, an LscanH-10-1064 (*2*) (AtekoTM, Russia) two-mirror galvanic scanning head with a lens providing a focus spot diameter of 30 μm is used. The donor and acceptor plates are 1 mm apart. Relative positioning of the laser head and plates is performed by an automated three-coordinate translation stage (*3*). The donor glass plate

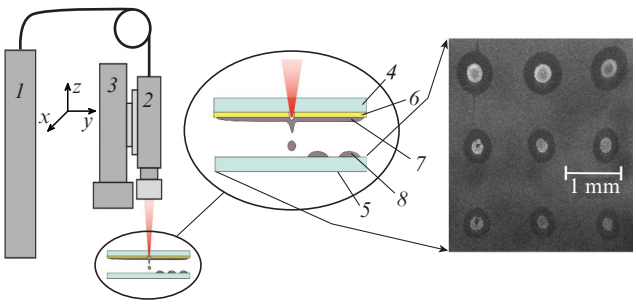

Figure 1. Setup for laser printing of microorganisms: (*1*) ytterbium fibre laser; (*2*) optical beam shaper; (*3*) three-coordinate translation stage; (*4*) donor plate; (*5*) acceptor plate; (*6*) metal coating; (*7*) gel layer with microorganisms; (*8*) microdroplets formed during transfer. On the right is the SEM image of a matrix of the substance of crystallised microdroplets on the acceptor plate.

V.P. Zarubin National University of Science and Technology 'MISiS', Leninsky prosp. 4, 119049 Moscow, Russia,
e-mail: zarubin.vasily@gmail.com;
V.S. Zhigarkov, V.I. Yusupov Institute of Photon Technologies, Federal Scientific Research Centre 'Crystallography and Photonics', Russian Academy of Sciences, ul. Pionerskaya 2, 108840 Moscow, Troitsk, Russia; e-mail: vzhigarkov@gmail.com;
A.A. Karabutov Institute of Laser and Information Technologies, Russian Academy of Sciences, ul. Svyatoozerskaya 1, 140700 Shatura, Moscow region, Russia; International Laser Centre, Lomonosov Moscow State University, Vorob'evy Gory 1, 119991 Moscow, Russia

Received 19 June 2019; revision received 16 September 2019
Kvantovaya Elektronika **49** (11) 1068–1073 (2019)
Translated by M.A. Monastyrskiy

is coated with a layer of metal (gold, chrome and titanium coatings are used) with a thickness of 50 nm, and the metal – with a gel layer having a thickness of 200 ± 30 μm, which is applied using a special device. The gel is a 2% aqueous solution of hyaluronic acid. All systems used in the work are synchronised. The process of laser exposure is controlled by a personal computer. An example of the image of the thus obtained matrices is shown in Fig. 1. Dark spots correspond to dried gel droplets, white spots – to crystallisation centres of gel content. Note that the droplet size can vary widely by changing the system parameters (film material, gel layer thickness, energy and pulse duration, etc.). Further study of the printing process was carried out on the example of a gold-coated donor plate.

3. Acoustic response of laser printing

One of the values characterising the transfer process is the pressure of acoustic waves excited during heating and destruction of the metal film [25]. Under the action of high-intensity laser radiation, shock acoustic waves can arise, which, however, quickly decay and pass over to a linear regime at distances of ~200 μm [26]. The smallness of this distance makes it necessary to use optical methods for studying such shock waves, in particular, shadowgraphy, the implementation of which is rather complicated. In this regard, in the present work, the assessment of the characteristics and qualitative description of the ongoing processes were conducted on the basis of measurements of the acoustic field in the far zone using a hydrophone [26, 27].

Acoustic pulses excited by nanosecond laser radiation have a wide spectral band (from 100 kHz to 100 MHz and higher) [28]; therefore, for their registration, a high-frequency broadband coaxial hydrophone (Fig. 2) based on a $LiNbO_3$ crystal was used. The distinctive feature of such receivers is their high sensitivity in a wide (1–100 MHz) frequency band and the presence of a narrow time diagnostic window that enables recording of pulses with a duration up to ~1 μs (which is determined by the crystal length of 6 mm [29]).

To obtain numerical values characterising the acoustic pressure recorded in the far zone, amplitude calibration of a broadband hydrophone is required. The difficulty of calibrating such receivers is the need for a broadband source and a receiver with known spectral characteristics. Optoacoustic sources are broadband sources with a well-repeated and accurately calculated pulse shape [28]; therefore, in this work, a photoacoustic ultrasound source was produced using a stable Nd:YAG laser (pulse duration, 8 ns; wavelength, 1064 nm; tunable pulse energy, 1–20 mJ; Quantel, USA) and a SZS-22 light filter absorbing laser radiation and exciting ultrasound due to the thermoelastic effect. The spectral band of the excited ultrasound is 0.1–20 MHz. A piezopolymer needle hydrophone based on polyvinylidene fluoride with a sensing element diameter of 1 mm and a reception band of 0.5–15 MHz (Precision Acoustics, United Kingdom) was used as a calibrated receiver.

For calibration, a series of measurements of acoustic signals by two hydrophones at different laser pulse energies was conducted. In each measurement, the waveforms (Fig. 3) of pulses received by both hydrophones were recorded and the amplitudes of the second peaks were measured, which carried the basic information about the excited signal. The first spurious recorded peak (Fig. 3b) occurs when an ultrasonic pulse crosses the front surface of a lithium niobate crystal, and has a small amplitude. The second peak is formed when the pulse crosses the back surface of the crystal. The rest of the signal can be considered spurious: it consists of various kinds of re-reflections inside the crystal.

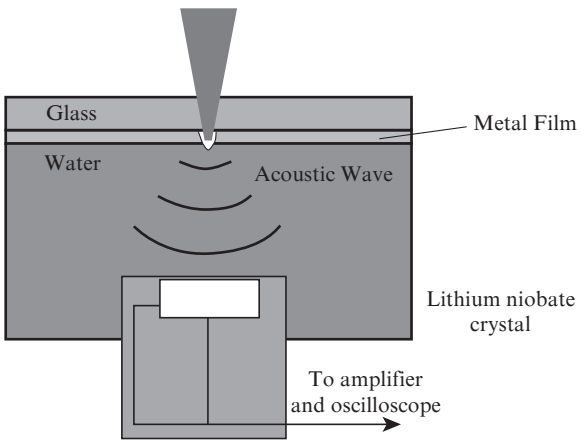

Figure 2. Scheme of recording the acoustic response of laser printing using a broadband acoustic receiver.

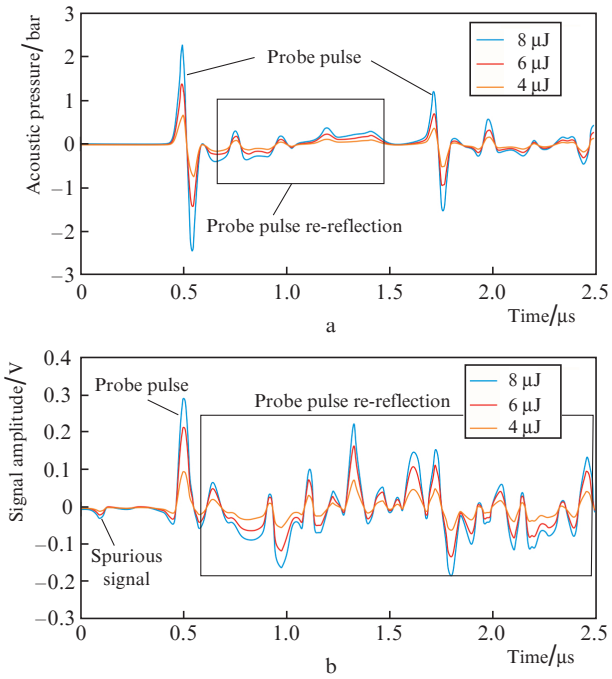

Figure 3. (Colour online) Examples of acoustic signals recorded during the calibration of a broadband hydrophone using laser pulses with different energies: (a) signal from the needle hydrophone and (b) signal from the broadband hydrophone.

The dependence of the amplitude of the signals recorded by the broadband hydrophone on the amplitude of the signals recorded by the needle hydrophone was linear, and so the least square approximation of data was used to obtain the calibration coefficient. The frequency bands of both hydrophones and the source are different, but they have overlapping parts. In this regard, before determining the signal amplitudes, their filtering was used to isolate the signal com-

ponents in the common frequency band 2–12 MHz. Thus, narrowband calibration of the broadband receiver allowed us to obtain accurate results due to sufficient uniformity of spectral characteristics of the receiver based on a lithium niobate crystal [29].

To measure the acoustic response during laser printing, a broadband hydrophone was placed in water, opposite to the place of laser irradiation of the gold coating of the donor plate at a distance $z \sim 30$ mm from it, which corresponds to the far zone of acoustic radiation (the diameter of the laser spot on the absorbing film was 30 μm). A series of experiments was conducted to measure the dependence of the amplitude of acoustic pulses on the laser pulse energies $E \approx 5–100$ μJ for durations $\tau_{las} = 8$ and 14 ns. To evaluate the pressure in the immediate vicinity of the film, data were recalculated according to the Gaussian beam formula [29] $P_a = p_{exp}\sqrt{1 + (\lambda_0 z/\pi r^2)^2}$, where $r \approx 15$ μm is the initial beam radius; p_{exp} is the pressure measured in the far zone; $\lambda_0 = c_0\tau_{las}$ is the characteristic wavelength of acoustic radiation; and $c_0 = 1500$ m s^{-1} is the speed of sound in water. The results presented in Fig. 4 show that the dependence of the acoustic response amplitude on the laser pulse energy is linear with good accuracy, and the acoustic pressure amplitude weakly depends on the duration of the laser pulses in the range of 8–14 ns. The maximum pressure amplitude was ~500 bar. When a plane wave propagates in water, such amplitudes correspond to a nonlinear propagation regime. However, in this case, the transverse size of the excitation region of the sound beam is small and diffraction is the predominant process. Therefore, the waveform is closest to spherical, and for such waves, as is known [30], nonlinear effects are much weaker than those for plane waves. In this regard, consideration of the propagation of waves outside the region of their excitation in the linear regime does not lead to significant errors in the estimates.

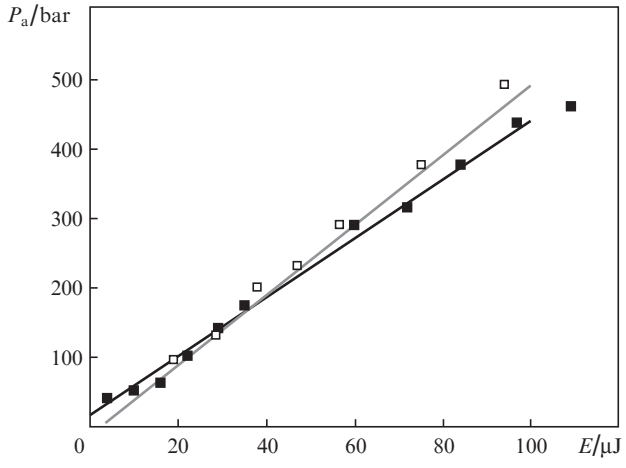

Figure 4. Acoustic response amplitude P_a of the system as a function of the laser pulse energy E at τ_{las} = (■) 8 and (□)14 ns.

Note that the negative effect of the acoustic wave on microbiological living systems depends on both the wave amplitude and its frequency. An increase in both parameters leads to an increase in the forces deforming microorganisms. In the operating range of laser pulse energies, the pressure amplitude reaches several hundred bars in the gel volume, and the characteristic wavelength of acoustic radiation is $\lambda = c_0\tau_{las} \approx 15$ μm, which is larger or comparable to the size of many microorganisms. The assessment of the influence degree of acoustic pressure can be based on the fact that in acoustic microscopy of microorganisms and other similar methods, high-frequency nondestructive acoustic radiation with higher frequency is used, the pressure amplitude of which is comparable to the pressure estimates obtained in this work for the operating regime [31].

4. Transfer processes and their impact on living systems

Physical processes occurring in a metal film during the laser radiation absorption should be considered at different time scales [32]. The main absorber of laser radiation in metals is the electron gas. In this case, the temperature of the electron gas and crystal lattice is equalised as a result of electron–phonon relaxation during the times of $\sim 10^{-11}$ s. After that, the equations of equilibrium thermodynamics become applicable. The most important factor that actually determines all physical processes during laser printing of microdroplets is the heat transfer in the glass substrate–film–liquid system. The time of heat redistribution over the film thickness can be estimated as $\tau_{tl} = h_g^2/\chi_g \approx 20$ ps, where χ_g is the thermal diffusivity of gold and $h_g = 50$ nm is the gold deposition thickness. The heat propagation time in the film plane can be estimated similarly: $\tau_{tt} = r^2/\chi_g \approx 2$ μs. Thus, at $\tau_{las} \approx 10$ ns, the inequality $\tau_{tl} \ll \tau_{las} \ll \tau_{tt}$ is satisfied, and heat propagates mainly perpendicular to the film plane. To calculate the fractions of radiation energy absorbed (γ) and transmitted (t) through a metal film, we can use the formula for the case of a film that is thin compared to the wavelength ($h_g = 50$ nm $\ll$ 1064 nm) [33]; these fractions constitute ~0.03 and ~0.05, respectively.

The thicknesses of the heated layers of the glass substrate and water during the laser pulse action are as follows: $h_{gl} = \sqrt{\tau_{las}\chi_{gl}} \sim 60$ nm, $h_w = \sqrt{\tau_{las}\chi_w} \sim 40$ nm, where χ_{gl} and χ_w are the thermal diffusivities of glass and water. Then the average temperature in this area can be estimated from above as follows:

$$T_a = \frac{\gamma E}{\pi r^2(\rho_{gl}h_{gl}c_{gl} + \rho_w h_w c_w + \rho_g h_g c_g)} \sim 1000 \text{ K},$$

where $E = 30$ μJ is the laser pulse energy; c_{gl}, c_w and c_g are the heat capacities of glass, water and gold; and ρ_{gl}, ρ_w and ρ_g are the densities of these substances. Thus, a really high temperature is reached near the metal film; however, due to the high heat capacity of gel, the temperature of areas distant a few micrometers from the metal film is only slightly higher than the temperature of the ambient medium. Thus, the resulting temperatures practically do not damage the biological material during laser printing.

Strong and rapid heating of the liquid near the metal film causes its explosive boiling and the formation of a rapidly expanding vapour bubble. In this case, a gel jet appears, transferring the substance to the acceptor plate. In some works [5, 34, 35], the laser-induced formation of gel jets near the free surface of the liquid was experimentally studied and numerically analysed. These results can be used to illustrate the jet formation in our case as well. As a result of explosive boiling, a small vapour bubble rapidly expanding towards the free surface is formed, along the wall of which a pressure gradient arises, leading to the appearance of external gel flows from the bubble periphery to its apex. The interaction of these flows leads to the appearance of a jet and a counter-jet in the

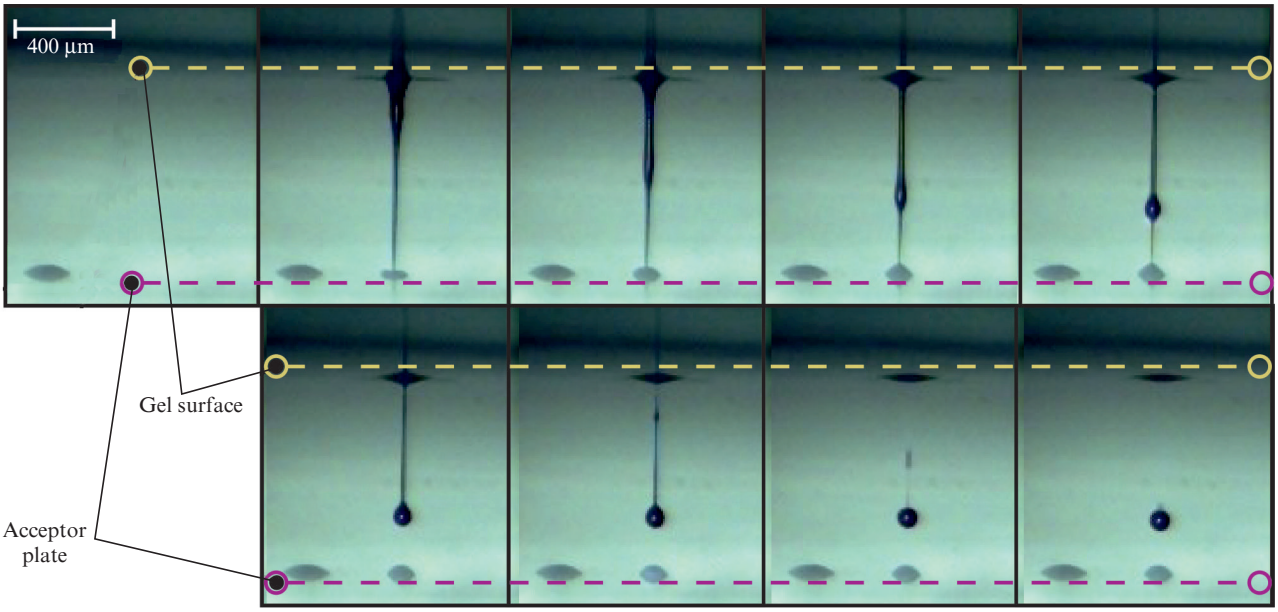

Figure 5. Process of the microdroplet formation on the acceptor plate, recorded by a high-speed camera (10000 frames per second) at $E = 30$ µJ, $\tau_{las} = 8$ ns.

apex region. Depending on the regime used, the jet can then break away from the bubble wall, continue its independent motion towards the acceptor plate and disintegrate into several fragments or start moving in the opposite direction and completely absorb into the gel layer. The main factors determining the regime of emerging flows are the viscous and thermal properties of the liquid, the amount of energy absorbed by the plate and thermal properties of the metal deposition.

To study the regimes of occurrence of such jets, optical recording of the process of their formation was conducted using a Fastcam SA-3 high-speed camera (recording speed up to 100000 frames per second; Photron, Japan). In the course of high-speed imaging, illumination was performed by radiation from a cw laser at a wavelength of 660 nm, with the formation of a beam using a telescopic system. The recorded transfer process is shown in Fig. 5. In the operating regime, a droplet is formed in two stages. At the first stage (second frame in Fig. 5) a small volume of substance is transferred with a large acceleration ($\sim 10^5$ m s^{-2}, calculated on the basis of the frames obtained). At the second stage (from the third to the last frame in Fig. 5), a bulk of the substance is transferred with much lower acceleration (~ 5000 m s^{-2}). From the viewpoint of the microorganism survival rate, such dynamic loads are not a critical obstacle for laser printing: for example, in work [36] it was shown that the survival rate of a number of bacterial organisms at accelerations being several orders of magnitude greater is close to 100%.

Another factor that can significantly affect the survival of bacteria is the presence of micro-and nanoparticles of metal in the microdroplets formed during laser printing. There are several mechanisms of the metal film destruction, associated with melting, evaporation and mechanical 'splitting' of metal. It is these mechanisms that determine the size of the particles formed. The initial motion of fused gold is determined by the stresses in metal, which must exceed the adhesion force of the fused film, the surface tension of the fused metal and the external pressure from the gel. This motion leads to the removal of part of the film material and its transfer in gel droplets to the acceptor plate. As can be seen in the SEM images of the holes formed in the film under laser irradiation (Fig. 6), the extreme fused part of these holes peels off. This is because the material is removed along the melting boundary due to mechanical stresses caused by the relatively weak adhesion of the deposited gold to the glass substrate. Thus, the material of the metal film from its central region breaks away with great speed from the surface, pulling out the edge areas behind it. The resulting nonuniformity of the fused edges is due to the nonuniformity of the film adhesion and the nonuniformity of laser illumination. A significant amount of gold is present in the central part (the zone of the greatest impact), which can be explained by the fusion of part of the glass substrate and the remaining gold particles.

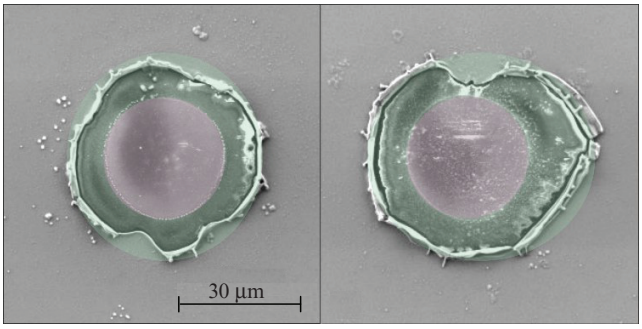

Figure 6. SEM images of the holes formed under irradiation of a gold film by pulses with $\tau_{las} = 8$ ns and $E =$ (a) 10 and (b) 30 µJ.

A significant number of works is dedicated to the study of toxicity of gold particles (and other metals) in relation to various microorganisms. It can be noted that the most important factors determining toxicity are the size and concentration of these particles [37, 38]. The maximum concen-

tration of gold in microdroplets in the present work can be estimated as 50–100 μM (under the condition of complete transfer of gold from the laser irradiation region). In this case, as follows from the results of electron microscopy, particle sizes are in the micro- and nanometre ranges. As is known (see, for example, [38]), depending on the particle size distribution, such concentrations of gold particles can lead to an increase in the metal content directly in microorganisms. This has a toxic effect on some microorganisms, others are more resistant.

Another factor to consider is the high density of electromagnetic radiation. Previous experimental studies have shown [24] that up to ~15% of laser energy, or 0.2–0.6 J cm^{-2} in the operating energy range, passes through the gold film during laser printing. Pulsed radiation with a wavelength of 1064 nm used in this work is poorly absorbed by cell elements, and therefore its impact on microscopic living systems, even at doses close to the operating ones, should not lead to irreversible changes. Thus, Sengupta et al. [39] showed that exposure of human cells to 600 consecutive radiation pulses of 5–9 ns duration with a wavelength of 1064 nm at a dose of 0.2 J cm^{-2} leaves ~90% of cells viable even with addition of carbon-absorbing nanoparticles. Kim et al. [40] established that the impact on Escherichia coli of pulsed laser radiation with a wavelength of 1064 nm at a dose of 3 J cm^{-2} did not lead to changes in 95% of cells.

However, the influence of most of these factors on various types of microorganisms can be significantly different, and so it is necessary to consider the efficiency of laser printing for each specific species. The laser printing setup presented in this work was used to isolate microorganisms from the soil [41]. It is shown that laser printing really allows one to increase the number of cultivated microorganisms compared to traditional methods while maintaining a high viability of organisms. The use of laser printing has led to an increase in the number of genera of isolated bacteria of both gram-negative and gram-positive groups that have not been cultivated before by standard methods. In this case, a representative of the rare genus Nonomurea was isolated from the soil without the use of sophisticated selective media and the addition of cocktails with antibiotics.

5. Conclusions

Thus, we have evaluated the parameters of physical processes that occur during laser printing of gel droplets and are the most harmful to microorganisms. For this purpose, a methodology has been developed for evaluating the acoustic pressure arising in the field of laser printing using a broadband hydrophone based on a lithium niobate crystal. According to the results obtained, the pressure amplitude in the gel layer reaches several hundred bars. Dynamic loads arising in the processes of temperature transfer and the concentration of metal particles in the droplets have been estimated. The results obtained have been compared with the data on the survival of microorganisms, known from the literature. The comparison has shown that factors negatively affecting microorganisms do not limit the prospects of the developed printing method. This conclusion is consistent with successful biological experiments on the transfer and cultivation of individual bacterial organisms.

Acknowledgements. This work was supported by the Ministry of Science and Higher Education within the State Assignment of FSRC 'Crystallography and Photonics', RAS, in part of the development of the cell printing technology and by the Russian Foundation For Basic Research (Project Nos 18-32-00607 and 18-29-06056) in part of studying laser-induced transfer processes.

References

1. Pique A., Chrisey D.B., Auyeung R.C., Fitz-Gerald J., et al. *Appl. Phys. A*, **69**, S279 (1999).
2. Pique A., Auyeung R.C., Kim H., Metkus K.M., Mathews S.A. *J. Laser Micro Nanoen.*, **3**, 163 (2008).
3. Narazaki A., Sato T., Kurosaki R., Kawaguchi Y., Niino H. *Appl. Phys. Express*, **1**, 057001 (2008).
4. Suzuki K. *Electr. Eng. Jpn.*, **165**, 60 (2008).
5. Unger C., Gruene M., Koch L., Koch J., Chichkov B.N. *Appl. Phys. A*, **103**, 271 (2011).
6. Kuznetsov A.I., Unger C., Koch J., Chichkov B.N. *Appl. Phys. A*, **106**, 479 (2012).
7. Auyeung R.C., Kim H., Mathews S., Pique A. *Appl. Opt.*, **54**, F70 (2015).
8. Ma H., Mismar W., Wang Y., Small D.W., et al. *J. Royal Soc. Interface*, **9**, 1156 (2011).
9. Chatzipetrou M., Tsekenis G., Tsouri V., Chtzandroulis S., Zergioti I. *Appl. Surf. Sci.*, **278**, 250 (2013).
10. Koch L., Kuhn S., Sorg H., Gruene M., et al. *Tissue Eng. Part C Methods*, **16**, 847 (2009).
11. Nguyen A.K., Narayan R.J. *Ann. Biomed. Eng.*, **45**, 84 (2017).
12. Ovsiannokov A., Gruene M., Pflaum M., Koch L., et al. *Biofabrication*, **2**, 014104 (2004).
13. Serra P., Colina M., Fernandez-Pradas J.M. *Appl. Phys. Lett.*, **85**, 1639 (2004).
14. Park M.A., Jang H.J., Sirotkin F.V., Yoh J.J. *Opt. Lett.*, **37**, 3894 (2012).
15. Baxter J., Mitragotri S. *Expert Rev. Med. Devices*, **3**, 565 (2006).
16. Martin G.D., Hoath S.D., Hutchings I.M. *J. Phys. Conf. Ser.*, **105**, 012001 (2008).
17. Ringeisen B.R., Rincon K., Fitzgerald L.A., Fulmer P.A., et al. *Methods Ecol. Evol.*, **6**, 209 (2015).
18. Yusupov V.I., Gorlenko M.V., Cheptsov V.S., Minaev N.V., et. al. *Laser Phys. Lett.*, **15**, 0656054 (2018).
19. Pohl R., Visser C.W., Romer G.W., Lohse D., Sun C., Huis B. *Phys. Rev. Appl.*, **3**, 024001 (2015).
20. Brasz C.F., Yang J.H., Arnold C.B. *Microfluid. Nanofluidics*, **18**, 185 (2015).
21. Delaporte P., Alloncle A.P. *Opt. Laser Technol.*, **78**, 33 (2016).
22. Biver E., Rapp L., Alloncle A.P., Delaporte P. *Appl. Surf. Sci.*, **302**, 153 (2014).
23. Duocastella M., Fernandez-Pradas J.M., Morenza J.L., Serra P. *Jpn. J. Appl. Phys.*, **106**, 084907 (2009).
24. Yusupov V.I., Zhigar'kov V.S., Churbanova E.S., et al. *Quantum Electron.*, **47**, 1158 (2017) [*Kvantovaya Elektron.*, **47**, 1158 (2017)].
25. Samokhin A.A., Shashkov E.V., Vorobiev N.S., Zubko A.E. *Pis'ma Zh. Eksp. Teor. Fiz.*, **108** (6), 388 (2018).
26. Vogel A., Busch S., Parlitz U. *J. Acoust. Soc. Am.*, **100**, 148 (1996).
27. Pushkin A.V., Bychkov A.S., Karabutov A.A., Potemkin F.V. *Laser Phys. Lett.*, **15**, 065401 6 (2018).
28. Gusev V.E., Karabutov A.A. *Laser Optoacoustics* (New York: AIP, 1993).
29. Oraevsky A.A., Karabutov A.A. *Proc. SPIE*, **3916**, 228 (2000).
30. Krasil'nikov V.A., Krylov V.V. *Vvedeniye v fizicheskuyu akustiku* (Introduction to Physical Acoustics) (Moscow: Nauka, 1984).
31. Augustsson P., Karlsen J.T., Su H.W., Bruus H., Voldman J. *Nat. Commun.*, **7**, 11556 (2016).
32. Ivochkin A.Y., Kaptilniy A.G., Karabutov A.A., Ksenofontov D.M. *Laser Phys.*, **22**, 1220 (2012).
33. Abeles F. *J. Opt. Soc. Am.*, **47**, 473 (1957).
34. Mezel C., Soquet A., Hallo L., Guillemot F. *Biofabrication*, **2**, 014103 (2010).

35. Pearson A., Cox E., Blake J.R., Otto S.R. *Eng. Anal. Bound. Elem.*, **28**, 295 (2004).
36. Mastrapa R.M.E., Glanzberg H., Head J.N., Melosh H.J., Nicholson W.L. *Earth Planet Sci. Lett*., **189**, 1 (2001).
37. Chithrani B.D., Ghazani A.A., Chan W.C. *Nano Lett*., **6**, 662 (2006).
38. Alkilany A.M., Murphy C.J. *J. Nanopart. Res*., **12**, 2313 (2010).
39. Sengupta A., Kelly S.C., Dwivedi N., Thadhani N., Prausnitz M.R. *ACS Nano*, **8**, 2889 (2014).
40. Kim J.W., Shashkov E.V., Galanzha E.I., Kotagiri N., Zharov V.P. *Laser Surg. Med*., **39**, 622 (2007).
41. Gorlenko M.V., Chutko E.A., Churbanova E.S., Minaev N.V., et al. *J. Biol. Eng*., **12**, 27 (2018).